CO9-1 Leaching behavior of fission products from simulated MCCI debris

T. Sasaki, N. Sato[1], A. Kirishima[1], D. Akiyama[1], T. Kobayashi, K. Takamiya[2], S. Sekimoto[2], Y. Kodama and Q. Zhao

Graduate School of Engineering, Kyoto University

[1] *Institute of Multidisciplinary Research for Advanced Materials, Tohoku University*

[2] *Institute for Integrated Radiation and Nuclear Science, Kyoto University*

INTRODUCTION: Under the high-temperature conditions in the reactor cores of the Fukushima Daiichi Nuclear Power Station (FDNPS) during the accident, UO_2, zircaloy, and structural materials such as concrete are thought to be reacted [1]. Uranium and these elements in the fuel debris could take various chemical states depending on chemical conditions to which they were exposed. Therefore, the aging degradation of fuel components contacting with water would be investigated to evaluate the long-term stability. Several fission products (FPs) have been produced by short-time neutron irradiation of simulated debris, which was synthesized by heat treatment of MCCI debris under reducing and oxidizing conditions. The leaching ratio of elements such as Zr, Ru, I, and Ba would be a proportional relationship with that of uranium or Cs as a matrix or a major FP, respectively, under various solution conditions.

EXPERIMENTS: In the preparation of MCCI debris, U:Zr was assumed to be 5:1, as a typical combination of UO_2 fuel and oxidized zircaloy-clad. The mixing ratios of cement intended to be shortage and excess amount of Ca to U; 1:0.75, 1:1.75, and 1:6.75. The mixture was heated at 1200°C for 2 hours under a reducing (10% H_2) and oxidizing (2% O_2) atmosphere — called as #R and #O series. During furnace cooling, pure argon gas was kept flowing. After the cooling, the sample was investigated by XRD. The simulated MCCI debris sealed in a quartz ampoule was inserted into a polyethylene capsule and irradiated using Pn-2 of Kyoto University Reactor. The gamma-ray activity, which is considered as an initial inventory of each radionuclide in the solid sample, was measured using a Ge detector after cooling in order to allow for the decay of highly radioactive, short-lived nuclides.

RESULTS: Under reducing heat treatment conditions of H_2 gas, Ca and SiO_2 did not react with UO_2, while Ca_3SiO_5 was assigned (a component of cement). The presence of ZrO_2, Ca zirconate was preferentially produced. Under oxidizing heat treatment conditions O_2 gas, dominant phase (w/o cement) was U_3O_8, and the solid solution was partly observed. The presence of less Ca to U (1:0.75), cubic-fluorite-type solid solutions formed, and in the presence of excess Ca, trigonal $CaUO_4$ (1.75), and Ca_3UO_6 (1:6.75) were obtained. Excess Ca was produced Ca silicate (Ca_2SiO_4) and Ca zirconate ($CaZrO_3$) similar to #R. Thus, Ca reacted with U preferentially compared to Zr and Si, forming a Ca-rich uranate with increasing Ca:U ratio.

Fig. 1. Typical appearance of simulated MCCI debris prepared under reducing conditions.

Five FPs were mainly produced by thermal-neutron irradiation. Static leaching test was done by using 0.1 M $NaClO_4$ at pH 7. After 4 weeks shaking, the radioactivity or the molar concentration in filtrate were measured, and then the leaching ratio R [2] was evaluated.

The R_{Cs} values higher than those of UO_2 and U_3O_8, suggesting an induced leaching due to Ca dissolution of MCCI debris or complexing U with CSH. Such speculation would be supported by R_{Cs}. The same trend was observed in I and Ba systems. Trace I as I^-, R_I showed a similar trend as Cs.

Compared to U compounds w/o Ca, most of R_M values of MCCI debris (at 1200°C) increased. Meanwhile, $\log R_{Ca}$ of #R series showed quite high order range of 3–5, whereas the values of #O were relatively low. This result would be because of the different predominant species of Ca between #R and #O. About trace Ba as Ba^{2+}, R_{Ba} showed the same trend as R_{Ca}. The R_{Ru} of #R and #O were slightly lower than others (except Zr), which is consistent with previous reports of $U(Zr)O_2$, although the chemical property is unknown. Most of R_{Zr} values could not be determined due to the quite low activity below the detection limit, corresponding to 10^{-15} M.

In conclusion, a mixture of cement components heated at 1200°C under H_2 and O_2 conditions formed UO_2 (unreacted) and calcium uranates, respectively. Under this specific condition, the excess Ca and Si could form $CaZrO_3$ and Ca_2SiO_4 (and CaO), which cause to increase pH in the present batch-wise tests. Significant increase of R_M was observed comparing with R_M in the absence of cement components. It is thought to be due to 1) an increase of the surface area of powder samples by matrix Ca dissolution, or 2) formation of U-CSH.

Combination of spectroscopic methods will give a new insight into the chemical property of debris before and after leaching test.

REFERENCES:

[1] T. Kitagaki *et al.*, J Nucl Mater., **486** (2017) 206-215.
[2] T. Sasaki *et al.*, J. Nucl Sci Technol., **53** (2016) 303-311.

CO9-2 Complex formation of zirconium with hydroxycarboxylic acids

T. Kobayashi, T. Sasaki, T. Saito[1], K. Takamiya[1], S. Sekimoto[1], M. Moniruzzaman, T. Fushimi, K. Haruki, and T. Suzuki

Graduate School of Engineering, Kyoto University
[1] Institute for Integrated Radiation and Nuclear Science, Kyoto University

INTRODUCTION: Tetravalent zirconium, Zr(IV), is known to undergo extensive hydrolysis in aqueous solution and its solubility is limited by a sparingly soluble amorphous hydroxide solid phase, $Zr(OH)_4$(am), in neutral to alkaline pH range. In the presence of suitable inorganic or organic ligands, Zr(IV) solubility is increased by the formation of soluble complexes. Enhanced Zr(IV) solubility is an issue in the environmental context of safe radioactive waste disposal, because the long half-life fission product ^{93}Zr ($T_{1/2}$=1.53×10^6 y) in radioactive waste forms Zr(IV) and can migrate with groundwater under the disposal conditions. Although a very few inorganic or organic ligands can compete with the strong hydrolysis reactions that occur in neutral to alkaline solutions, we have found that several poly(hydroxy)carboxylic acids formed stable complexes with Zr(IV) in neutral to alkaline solutions[1]. In the present study, we investigated the solubility of Zr(IV) in the presence of three simple hydroxycarboxylic acids (hydroxyacetic (glycolic, O20) and 3-hydroxypropionic (O21) to clarify the role of the hydroxy groups in Zr complexation. The Zr(IV) solubility dependence on hydrogen ion concentrations (pHc) and hydroxycarboxylic acid concentrations ($[L]_{tot}$) was examined to identify the dominant soluble species and to determine their formation constants.

EXPERIMENTS: Sample solutions were prepared by an undersaturation approach. An aliquot of $Zr(OH)_4$(am) stock suspension was added to sample solutions at selected pHc and $[L]_{tot}$ (L = O20 and O21, see Fig. 1) values within the pHc range of 7 to 13 and $[L]_{tot}$ range of 10^{-4} to 10^{-1} M. Sample solutions in polypropylene tubes were kept in the Ar-filled glove box and in some cases manually shaken for a few minutes. After given aging periods, the pHc of the sample solutions was measured and a 0.5-mL aliquot of the supernatant was passed through an ultrafiltration membrane (3kDa, pore size ~ 2 nm). The filtrate was acidified with 0.1 M nitric acid prior to the concentration measurements by inductively coupled plasma mass spectrometry (ICP-MS). The detection limit of Zr(IV) solubility was approximately $10^{-8.5}$ M.

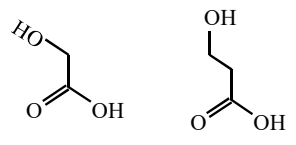

Hydroxyacetic (Glycolic) acid; O20 pK_a = 3.83 [2]

3-hydroxy-propionic acid; O21 pK_a = 4.61 [2]

Fig. 1. Hydroxycarboxylic acids used in this study.

RESULTS: Figure 2 shows the Zr(IV) solubility in the presence of 0.01 M and 0.1 M glycolic acid (O20) as a function of pHc, together with those in the absence of O20 [3,4]. The solubility in the presence of 0.1 M O20 equaled 10^{-7} M throughout the whole pHc range, and the solubility was about one order of magnitude higher than that in the absence of O20. Zr(IV)-O20 complexes were considered to be the predominant Zr(IV) species in 0.1 M O20 solution. Assuming that the solid phase retained its $Zr(OH)_4$(am) stoichiometry, the zero slope of the log [Zr] versus pHc plot indicated that the soluble Zr(IV)-O20 complex contained four OH groups in its chemical formula. Since the solubility increased monotonically with a slope of two at constant pHc levels, we assumed that $Zr(OH)_4(O20)_2^{2-}$ was the major species in the solution.

On the other hand, the Zr(IV) solubility in the presence of 0.01 M and 0.1 M 3-hydroxypropionic acid (O21) showed no significant increase from those in the absence of O21. This result suggested that complexation by O21 was not strong enough to solubilize Zr(IV) under the present experimental conditions. Zr(IV) chelation featuring 5-membered rings with O20 might be more stable than that with 6-membered rings with O21.

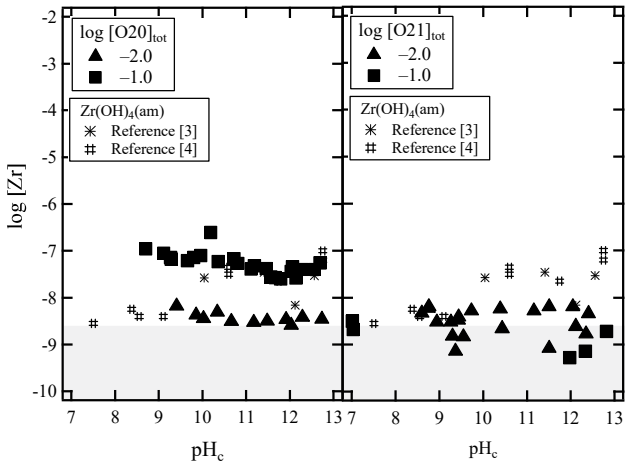

Fig. 2. Zr(IV) solubility in the presence of 0.01 M and 0.1 M O20 (left) and O21(right).

REFERENCES:

[1] T. Kobayashi *et al.*, J. Chem. Thermodynamics, **138** (2019) 151-158.
[2] R. M. Smith, NIST Critically Selected Stability Constants of Metal Complexes Database Version 5.0, Gaithersburg, USA (1998).
[3] T. Sasaki *et al.*, Radiochim. Acta, 94 (2009) 489-494.
[4] M. Altmaier *et al.*, Radiochim. Acta, 96 (2008) 541-550.

CO9-3 Electrodeposition Behaviors of Uranium and Aluminum on Copper Cathode in LiCl-KCl Eutectic Melts

Y. Sakamura, T. Murakami, K. Uozumi, M. Iizuka and K. Takamiya[1]

Central Research Institute of Electric Power Industry
[1]Institute for Integrated Radiation and Nuclear Science, Kyoto University

INTRODUCTION: Electrorefining in molten LiCl-KCl eutectic-based salts is the key separation process in the pyrochemical treatment of spent nuclear fuels [1,2]. It has been reported that Al cathode is suitable for collecting actinides in the form of intermetallic compounds with a high separation factor against rare-earth fission products [2]. Then, a chlorination process for the actinide-Al alloys using Cl_2 or HCl has been examined to separate volatile $AlCl_3$ from actinide chlorides [3,4]. A chemical reduction is subsequently conducted to obtain actinide metals [4].

We propose an electrorefining process to separate actinides from Al. Since U and Al simultaneously dissolve into LiCl-KCl eutectic melts during anodic dissolution of U-Al alloy [5], the separation between U and Al has to be conducted at cathode. The Al-Cu and U-Cu binary phase diagrams [6] suggest that Cu likely forms a stable alloy with Al but not with U. In the present study, electrodeposition behaviors of Al^{3+} and U^{3+} on Cu electrode in LiCl-KCl eutectic melts were investigated to evaluate the possibility of electrochemical separation between U and Al.

EXPERIMENTS: A LiCl-KCl eutectic melt was contained by a high-purity Al_2O_3 crucible at ~723 K, where a working electrode of Cu wire (1 mm diameter), a counter electrode of glassy carbon rod (3 mm diameter), a Ag/AgCl reference electrode and a type-K thermocouple were placed. The Ag/AgCl electrode consisted of a Ag wire immersed in a LiCl-KCl eutectic salt mixture with 1.0 wt% AgCl, which was contained in a closed-end Pyrex tube. The concentration of U^{3+} in the melt was increased by adding a prepared LiCl-KCl-UCl_3 salt whose U concentration was 11.4 wt% determined by ICP-AES analysis. $KAlCl_4$ (99.9% purity) obtained from APL Engineered Materials was used as a source of Al^{3+} ions because $AlCl_3$ is highly volatile. All the experiments using chlorides were conducted in a high-purity Ar atmosphere glove box (H_2O, O_2 < 1 ppm).

RESULTS: Figure 1 shows cyclic voltammograms (CVs) on Cu electrode in LiCl-KCl-UCl_3 and LiCl-KCl-$KAlCl_4$ melts. The CV in the LiCl-KCl-UCl_3 melt has a cathodic current peak at -1.46 V, which corresponds to the deposition of U metal. The sharp anodic current peak at -1.35 V is due to the dissolution of the deposited U metal. The redox potential of U^{3+}/U is in agreement with that previously reported [7]. There is no other distinct current peak, indicating that Cu forms hardly any alloys with U, which was verified in the temperature range 723-823 K.

The CV in the LiCl-KCl-$KAlCl_4$ melt has two distinct anodic peaks at -0.75 and -0.93 V, which are due to the dissolution of Al from Cu-Al alloy and Al metal, respectively. The cathodic peak at -0.90 V, corresponding to the anodic peak at -0.75 V, is due to the formation of Al-Cu alloy. The deposition of Al metal occurs at about -1.0 V [5]. The anodic peak at -0.65 V might be due to the Al dissolution from different Al-Cu alloys with less Al activity. The anodic current increasing at -0.40 V is due to the dissolution of Cu into the melt in the form of Cu^{+} ions.

CONCLUSIONS: The results of electrochemical measurements show that the difference in deposition potential on Cu between Al and U is 0.58 V, suggesting that Al is expected to be highly separated from U by using Cu as the cathode. Al electrodeposition tests in LiCl-KCl melts containing both Al^{3+} and U^{3+} will be conducted in the near future. The formation rate of Al-Cu alloy should be examined in detail, which may be affected by the operation temperature. The separation technique between U and Al investigated in this study can be applied to the treatment of irradiated U-Al alloy fuels.

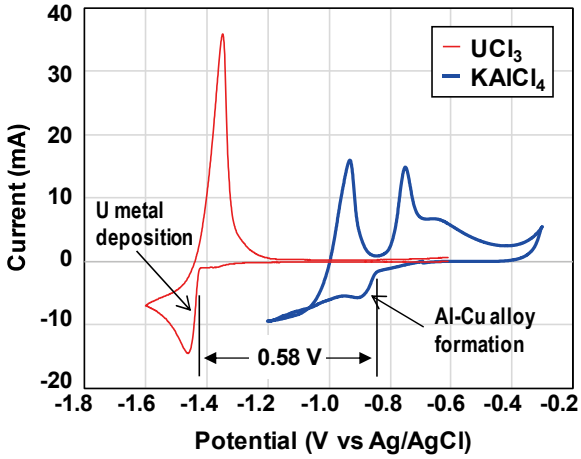

Fig. 1. Cyclic voltammograms obtained on Cu working electrode in LiCl-KCl-UCl_3 (0.16 mol% U) and LiCl-KCl-$KAlCl_4$ (0.099 mol% Al) melts at ~723 K. Scan rate 0.1 V/s.

REFERENCES:

[1] T. Murakami *et al.*, J. Nucl. Sci. Technol., **55** (2018) 1291.
[2] P. Soucek *et al.*, J. Nucl. Mater., **526** (2019) 151743.
[3] P. Soucek *et al.*, J. Nucl. Mater., **447** (2014) 38.
[4] R. Meier *et al.*, J. Nucl. Mater., **498** (2018) 213.
[5] Y. Sakamura *et al.*, KURRI Progress Report 2012, pp. 100.
[6] T. B. Massalski, *Binary Alloy Phase Diagrams*, Vol. 1, American Society for Metals, Metals Park, OH, 1986.
[7] Y. Sakamura *et al.*, J. Nucl. Mater., **502** (2018) 270.

CO9-4 Structural Change of Borosilicate Glass by Boron Isotope Composition

T. Nagai, Y. Okamoto, D. Akiyama[1], A. Uehara[2], T. Fujii[3], and S. Sekimoto[4]

Japan Atomic Energy Agency (JAEA)
[1]*Institute of Multidisciplinary Research for Advanced Materials (IMRAM), Tohoku University*
[2]*National Institute of Quantum and Radiological Science and Technology (QST)*
[3]*Graduate school of Engineering, Osaka University*
[4]*Institute for Integrated Radiation and Nuclear Science, Kyoto University*

INTRODUCTION: A high-level radioactive liquid waste from a reprocessing process for spent nuclear fuels is processed into a solidified waste made of a borosilicate glass. We estimated the Si-O bridging structure of neutron irradiated borosilicate glass by using Raman spectrometry, and confirmed that the Si-O non-bridging structure increased by the irradiation in our previous study [1]. The structural change by irradiation is regarded as the nuclear reaction $^{10}B(n,\alpha)^{7}Li$ studied by S. Peuget, et al [2], but the influence to a Si-O bridging structure by the boron isotope effect has not been clear.

In this study, to understand the influence of glass structural change by neutron irradiation and boron isotope composition, glass samples were made from enrichment boric acid reagents and neutron irradiation of those samples was carried out in Pn-2 of KUR. The structural change of glass sample after the irradiation will be investigated in 2020FY.

EXPERIMENTS: Three kinds of borosilicate glass of $17B_2O_3$-$65SiO_2$-$17Na_2O$-CeO_2-Nd_2O_3-Y_2O_3 were prepared from raw material reagents of SiO_2, Na_2CO_3, CeO_2, Nd_2O_3, Y_2O_3, and natural boric acid of H_3BO_3, enrichment boric acid of $H_3{}^{10}BO_3$ or $H_3{}^{11}BO_3$. These reagents were loaded in an alumina crucible and were melted at 1,150°C in an electric furnace. After the molten glass samples were solidified by cooling to room temperature, they were cut into thin plates. In this report, it is marked with ^{10}B-glass, natural-B-glass and ^{11}B-glass by kind of used isotopic boric acid reagents.

In Oct. of 2019, these thin plate samples were set in a polyethylene tube and were irradiated under the condition of 1,000 kW for 5, 10, and 20 min in the Pn-2 of KUR. After the radioactivity of the samples reduces to the background level, the Raman spectra of the samples will be measured by using a Raman spectrometer, NRS-3100 of JASCO in KUR.

Before neutron irradiation test of glass samples, the Si-O bridging structure difference by boron isotope composition compared by using a Raman spectrometry

RESULTS: The Raman spectrum of Si-O bridging structure of a silicate glass were in the wavenumber of 850-1200 cm^{-1}, and the peak positions of Raman shifts were different from the number of non-bridging oxygen, NBO, of the Si-O bridging structure [3]. The Raman shifts of borosilicate glass samples appear in similar wavenumber of 850-1,200 cm^{-1}. The Raman peak of Q^4 structure without NBO appeared in around 1,150 cm^{-1}, and those of Q^3, Q^2, and Q^1 structures with the NBO number = 1, 2, and 3 were in 1,090, 1,000, and 900 cm^{-1} respectively. The peaks of Q^2 and Q^3 structures can be subdivided into plural by the Si-O-X connecting state, and were divided into $Q^{2(1)}$, $Q^{2(2)}$, $Q^{3(1)}$, and $Q^{3(2)}$.

When the Raman shifts of ^{10}B-glass and ^{11}B-glass samples were compared, the difference was observed and the measured spectra were separated into six Gaussian waves as shown in Fig. 1. The Raman peaks of Q^1, $Q^{2(1)}$ and $Q^{2(2)}$ structures of ^{10}B-glass were higher than those of ^{11}B-glass, and those of $Q^{3(1)}$, $Q^{3(2)}$ and Q^4 structures of ^{10}B-glass were lower than those of ^{11}B-glass. It was presumed that Si-O non-bridging structure in the borosilicate glass increased with an increase of the ^{10}B percentage.

The cause of the difference in Raman spectra by boron isotope composition of borosilicate glass is unclear in the present, and an additional investigation is necessary.

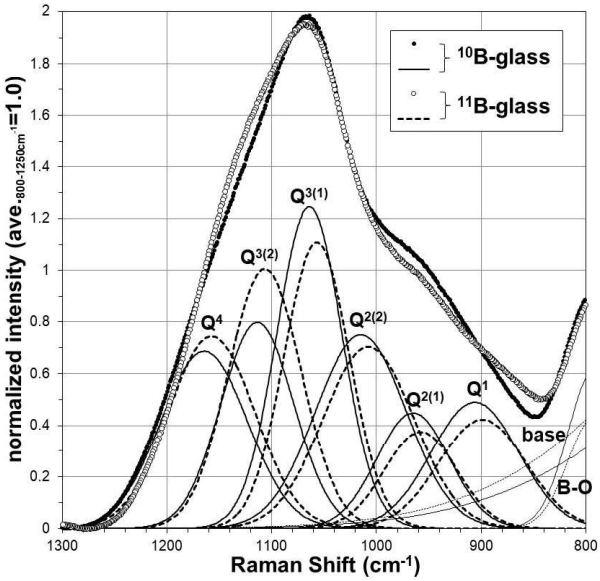

Fig. 1. Raman spectra and separated Gaussian waves. closed circles and fine lines are 10B-glass, and open circles and dotted lines are 11B-glass.

REFERENCES:

[1] T. Nagai, *et al*, 2018FY KURRI progress report, 30P10-7 (2019).
[2] S. Peuget, *et al,* Nucl. Inst. Methods in Phys. Res. B, **327** (2014) 22-28.
[3] P. McMillan, Am. Mineralogist, **69** (1984) 622-644.

CO9-5 Study on leaching behavior of carbon-14 from neutron irradiated stainless steel

R. Nakabayashi, S. Sekimoto[1], T. Sasaki[2], D. Sugiyama, T. Fujita

Radiation Safety Research Center, Nuclear Technology Research Laboratory, Central Research Institute of Electric Power Industry (CRIEPI)
[1]Institute for Integrated Radiation and Nuclear Science, Kyoto University
[2]Graduate School of Engineering, Kyoto University

INTRODUCTION: The speciation of ^{14}C released from low-level radioactive waste (irradiated stainless steel) is a key parameter in the safety assessment of the intermediate-depth disposal system in Japan. Most of the radionuclides released from the waste will sufficiently decay in the disposal facility owing to the multibarrier system. However, ^{14}C may not be retained in the multibarrier system until it sufficiently decays, depending on its chemical form. This indicates that it is necessary for the safety assessment to determine the chemical form of ^{14}C released from the waste under the disposal conditions (highly alkaline and low-oxygen conditions). To develop an understanding of the mechanism of release of ^{14}C from irradiated stainless steels, leaching experiments have been carried out using a non-irradiated stainless-steel powder in NaOH solutions (of approximately pH 12) under low-oxygen conditions [1, 2]. The results showed that the dominant chemical form of ^{12}C is a colloidal carbon. If the chemical form of ^{14}C released from the low-level waste under the disposal conditions is the colloidal carbons, most of the ^{14}C will be retained for sufficient time and decay in the disposal facility owing to the effect of the filtration property of the engineered barrier (i.e., bentonite). In the safety assessment, this can lead to a reduced dose derived from ^{14}C. It is essential to carefully determine the chemical forms and clarify why the colloidal carbons formed. In particular, there are few data for the ^{14}C species released from the irradiated stainless steel under the disposal condition. Therefore, the objective of this study is to identify the chemical form of ^{14}C released from the neutron irradiated stainless steel under the disposal conditions with the leaching experiments.

EXPERIMENTS: The type 316LN stainless-steel powder (particle size ranges from 20 to 53 μm, Lot No. F-1296, Sanyo Special Steel Co., Ltd., Japan was used in this study. The powder was produced by a gas atomization process. The process essentially consists of the atomization of a stream of liquid metal by high-pressure gas jets and nitrogen is taken into the metal as an impurity. The nitrogen content of the powder is 0.134 wt%, which were taken from a mill test report (No. 1385180011) provided by the suppliers. The chemical depth profile of the stainless-steel powder was obtained by scanning Auger electron spectroscopy/microscopy. The oxide thickness was estimated to be approximately 4 nm for the powder from half the decay of the oxygen content. The oxide layer is mainly composed of iron, chromium and nickel, which is similar to the surface characteristic of irradiated stainless steel generated by the operation of nuclear power plants [3]. The atomized powder (4 g) was packed in a quartz ampoule with 8 mm in diameter and 60 mm in depth and sealed by heating the top part of the ampoule in vacuo. These sealed ampoules were wrapped with aluminum foil and inserted into an aluminum capsule. Capsules containing the atomized powder were irradiated for 10 hours at 1 MW in Hyd facility of Kyoto University Reactor (KUR). The total amount of irradiated sample is 48 g. The thermal neutron flux was 1.63×10^{13} n cm^{-2} s^{-1} and the thermo neutron capture cross section for the $^{14}N(n,p)^{14}C$ reaction was 1.81×10^{-24} cm^{-2}.

RESULTS: In August of 2019, the samples were irradiated using Hyd facility of KUR. The samples irradiated for 10 hours are still cooled to allow for the decay of highly radioactive, short-lived nuclides. The ^{14}C inventory of irradiated sample was evaluated to be very low (~ 2.5×10^{3} Bq g^{-1}). The corrosion rate of this sample has not yet been clear. However, the corrosion rate of the type 316L stainless-steel powder, which is very similar to chemical composition of the type 316LN stainless-steel powder, in alkaline condition is extremely low (~ 1.5×10^{-13} m y^{-1}), according to previous studies [4]. Based on the above, the amount of ^{14}C species released from the irradiated steel during the leaching experiment is expected to be quite low and conventional radioanalytical techniques for ^{14}C detection (e.g., liquid scintillation counting) cannot detect the ^{14}C species in the leaching experiment. Therefore, a high-sensitivity analysis is planned to be carried out using accelerator mass spectrometry (AMS). AMS has a much lower detection limit than radioanalytical techniques because AMS does not depend on the disintegration of the radionuclide [5]. We plan to transfer the cooled samples to CRIEPI in order to carry out long-term leaching experiments in NaOH solutions under low-oxygen conditions. After the leaching experiments, we also plan to quantify the chemical species of ^{14}C in liquid and gas phases using AES.

REFERENCES:

[1] R. Nakabayashi and T. Fujita, MRS advances, **2** (2017) 597-602.
[2] R. Nakabayashi and T. Fujita, Radiocarbon, **60** (2018) 1691-1710.
[3] D. Bradbury *et al.*, Proceedings of International Joint Topical Meeting of the American Nuclear Society-Canadian Nuclear Association on the Decontamination of Nuclear Facilities. (1982).
[4] R. Nakabayashi and T. Fujita, Migration 2019, (2019) PA1-6.
[5] B. Z. Cvetković *et al.*, Radiocarbon, **60** (2018) 1711-1727.

CO9-6 Solvent extraction of selenium in the nitric acid solution with selected elements

T. Kawakami, Y. Yoneda, S. Ogawa, C. Kato, S. Fukutani[1], T. Matsumura[2], Y. Tsubata[2], K. Morita[2], A. Uehara[3], and T. Fujii
Graduate School of Engineering, Osaka University
[1]Institute for Integrated Radiation and Nuclear Science, Kyoto University
[2]Nuclear Science and Engineering Center, Japan Atomic Energy Agency
[3]National Institutes for Quantum and Radiological Science and Technology

INTRODUCTION: As a method to preserve high level waste from spent nuclear fuel, vitrification followed by geological deposition is considered. High level waste contains long-lived fission products (LLFP), with some that have a half-life of over 1,000,000 years. ^{79}Se is a LLFP with a half-life of 326,000 years and compared to other LLFP and minor actinides (MA), its toxicity appears earlier. Due to the half-life of ^{79}Se, it does not pose as an immediate risk, but considering geological deposition, it would be beneficial to separate and transmutate Se before the disposal. Selenium is also a rare earth element, and is used for glass manufacturing and Li-Se batteries. The separation and conversion method to reduce the long-term toxicity of LLFP is considered in previous studies using novel extractants [1]. However, the solvent extraction behavior of Se is not well known with these extractants. In this study, we focused on the separation of Se and the solvent extraction characteristics in a nitric acid system using novel extractants proposed for the SELECT process to understand the behavior of Se in the separation process of MA. Furthermore, we used extractants that are known to extract Se separately [2], and test whether it is possible to achieve high distribution ratios with co-existence of other elements simulating the high-level radioactive waste solution.

EXPERIMENTS: For the organic phase, *N, N, N′, N′, N″, N″*-hexaoctylnitrilotriacetamide (HONTA), alkyl diamide amine (ADAAM), *N, N, N′, N′*-tetradodecyl-diglycol amide (TDdDGA), *N*-phenyl ethylenediamine (*N*-PDA), *o*-phenylenediamine (*o*-PDA), and 4,5-dimethyl-1,2-phenylenediamine (DMePDA) were used as extractants and n-dodecane, 1-octanol and nitrobenzene were used as solvents. Tetravalent Se was dissolved in HNO_3 for the aqueous phase. For the simulation of high-level radioactive liquid waste, La was selected as a representative element of light lanthanides, Dy as a representative of heavy lanthanides, and Gd due to having an intermediate mass. In addition, Pd as a platinum group element in fission products, and Sr and Cs, which are elements with a large abundance in the liquid waste. The concentration of each element in the simulated solution are as follows: Se 1 mM, Pd 10 mM, Cs 15 mM, Sr 2.5 mM, Gd 1 mM, La 10 mM, Dy 1 mM. Both phases were stirred for 30 minutes to perform fore extraction, and then separated by centrifugation at 2000 rpm for 5 mins. Thereafter, HNO_3 was added to the separated organic phase to perform back extraction. All experiments were carried out at 298 K. The Se concentration of the aqueous phase after both extractions were measured by Inductively Coupled Plasma-Atomic Emission Spectrometry (ICP-AES) and Inductively Coupled Plasma-Mass Spectrometry (ICP-MS), and the distribution ratios were determined.

RESULTS: The distribution ratio of Se between HNO_3 and the organic phases of HONTA, ADAAM and TDdDGA was well below 1. Using *o*-PDA as the extractant with octanol, and high concentration HNO_3 for back extraction had the highest distribution ratio (D = 3.6). Using this condition, the distribution behavior of Se with multiple elements was observed (Fig 1). In the low nitric acid concentration, it was D > 10 for Se, and the separation factor for each element exceeded 1000.

CONCLUSION: Se was not extracted by the novel extractants and remained in the residual solution. For the simple extraction of Se, it was effective to use *o*-PDA as the extractant, octanol as the solution, and concentrated nitric acid for back extraction. Se was effectively separated from other elements in the simulated solution at low HNO_3 concentration.

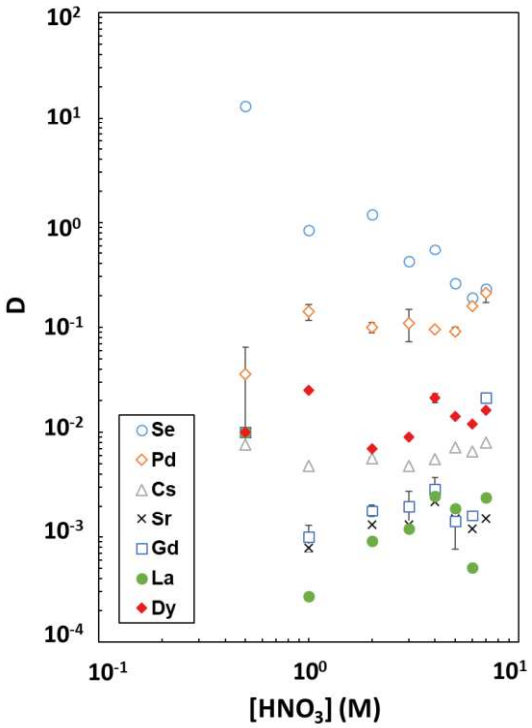

Fig. 1. Dependence of D on nitric acid concentration for selected elements using *o*-PDA.

REFERENCES:

[1] Y. Ban *et al.*, Solvent Extr. Ion Exch., **37** (2019) 27-37.
[2] Y. Sasaki *et al.*, Solvent Extr. Res. Dev. Jpn., **24** (2017) 113-122.

CO9-7 Effect of γ-Ray Irradiation in HNO_3 on Adsorptivity of Long-Chain 6-Membered Cyclic Monoamide Resin

Y. Yoshimura[1], R. Hamashiro[1], M. Nogami[1], and N. Sato[2]

[1]*Faculty of Science and Engineering, Kindai University*
[2]*Institute for Integrated Radiation and Nuclear Science, Kyoto University*

INTRODUCTION: It is of great importance to develop resins with selectivity to uranium(VI) species in nitric acid media. As a part of this purpose, we have been investigating the change in chemical structure and adsorptivity to metal ions of a cyclic monoamide resin. The manner of structure change in the resins has been found basically identical, namely, starting from the cleavage of the monoamide ring by the addition of oxygen atom originating from HNO_3, followed by the formation of chain monoamides by the continuous addition of oxygen. These compounds have multiple coordinative oxygen atoms, *e.g.*, carboxyl groups, but the change in the adsorptivity has been found different resulting probably from the number of atoms in the ring[1-3]. More recently, our attention has been paid to long-chain cyclic monoamides, and we have previously reported the results for the resin consisting of 1-(4-vinylbenzyl)piperidin-2-one (VBPP)[4]. It has a 6-membered cyclic piperidine ring with a spacer between the functional carbonyl group and the main polymer chain. In the present study, a newly synthesized long-chain cyclic monoamide resin consisting of 5-membered pyrrolidone ring (1-(4-vinylbenzyl)-pyrrolidone-2-one(VBPR)) was similarly investigated.

EXPERIMENTS: VBPR was synthesized by reacting 2-pyrrolidone with copolymer beads of chloromethylstyrene and divinylbenzene by following the literature[5]. γ-Ray irradiation to VBPR was carried out using 6 M HNO_3 similarly to the earlier study (max. 0.2 MGy)[1]. The irradiated VBPR was separated from the supernatant liquid and washed using distilled water to avoid further degradation by HNO_3. Adsorptivities of the irradiated VBPR to metal ions at equilibrium were obtained by a batch method. Samples of the conditioned resin (wet 0.15 g) and 3 cm^3 of 0.1 - 6 M HNO_3 solutions containing 1 mM Re(VI) or Zr(IV), or tracer U(VI) were shaken at 298K in a thermostatic shaking bath for 24 h. After shaking, samples of the supernatant were taken and the concentrations of the metal ions were measured using ICP-OES for Re and Zr, and ICP-MS for U. Adsorptivities were evaluated by the distribution ratio, K_d.

RESULTS: Adsorptivities of VBPR irradiated in 0.1 M HNO_3 at various dose to the examined metal ions are shown in Fig. 1. The K_d values for Re(VII) and Zr(IV) are found basically increased with increasing dose. For U(VI), the identical tendency is found for lower dose, and K_d values are found constant above 0.1 MGy. The K_d values for Re(VII) for VBPP were in an opposite manner decreased with increasing dose[4], and the reason remains unclear.

It is known that the bond between methylene carbon and nitrogen atom of tertiary-amine-type anion exchange resins undergoes cleavage by heating or γ-ray irradiation, leading to decrease in adsorptivity to metal ions. The results in Fig. 1 indicate that the reaction of the route (I) in Fig. 2 is dominant and that the route (II) is negligible in the present irradiation experiments. In fact, very little water-soluble organic compounds were detected by NMR analysis.

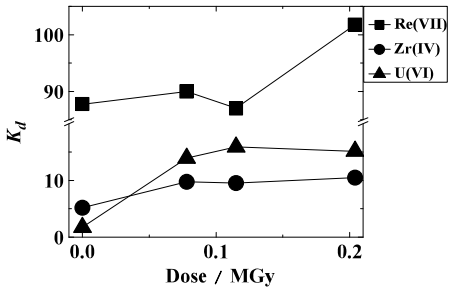

Fig. 1. Adsorptivity of VBPR irradiated in 6 M HNO_3 at various dose to metal ions in HNO_3

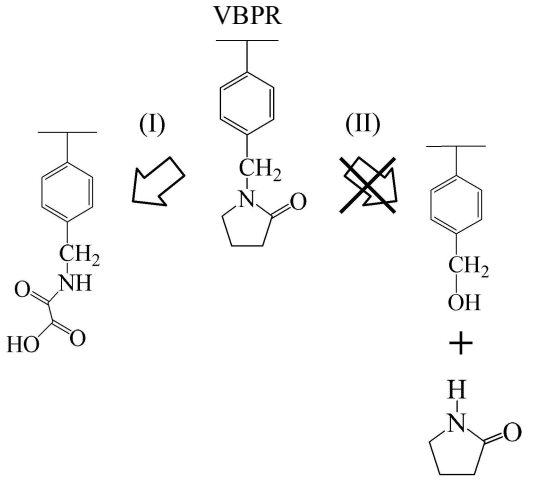

Fig.2. Expected major route of change in chemical structure of VBPR by γ-ray irradiation in HNO_3

REFERENCES:

[1] N. Miyata *et al.*, KURRI Progress Report 2010 (2011) 258.
[2] M. Nogami *et al.*, J. Radioanal. Nucl. Chem., **296** (2013) 423-427.
[3] T. Nishida *et al.*, KURRI Progress Report 2013 (2014) 295.
[4] M. Nogami *et al.*, KURRI Progress Report 2017 (2018) 197.
[5] M. Nogami *et al.*, Prog. Nucl. Energy, **50** (2008) 462-465.

CO9-8 Roll of Electrostatic Interaction in Attachment Process of Fission Products to Solution Aerosol Particles

K. Takamiya, Y. Takeuchi, T. Takeuchi, S. Sekimoto, Y. Oki and T. Ohtsuki

Institute for Integrated Radiation and Nuclear Science, Kyoto University

INTRODUCTION: A large amount of radioactive materials containing fission products have been released from the Fukushima Daiichi Nuclear Power Plant after the Great East Japan Earthquake in 2011. Main forms of the radioactive materials are insoluble micro-particles [1] and soluble aerosol particles. The generation processes of these materials are important to understand the environmental condition of the reactors. Experimental approach to elucidate the generation process of the radioactive aerosols has been performed in our previous work [2-5]. It was found that there is an attachment process induced by electrostatic interaction between a fission product and surface of an aerosol particle. However, the electrostatic interaction could not be quantitatively clarified because fission products emitted from ^{252}Cf source used in the previous work have recoil velocities which induces the attachment process by geometric collision. In the present work, the attachment behavior has been observed using aerosol generating apparatus combined with neutron irradiated UO_2 as a source of fission products. Since fission products released from the irradiated UO_2 by heating have no recoil velocity, observation of attachment behavior without geometric collisions becomes possible.

EXPERIMENTS: The experimental setup to generate and collect radioactive aerosols containing fission product is expressed in the previous report [6]. Powder of UO_2 was encapsulated in a quartz tube under reduced pressure, and the quartz tube covered by a polyethylene tube was inserted into polyethylene capsule to irradiate neutrons using pneumatic transport system, Pn-2, of KUR. The amount of UO_2 was 10 mg, and the neutron irradiation time is 30 min. A few mg of irradiated UO_2 powder was extracted to another quartz tube placed in an electric furnace. Fission products produced in the irradiated UO_2 powder was released by heating the furnace up to 1000°C. On the other hand, atomizer filled with 0.01 M sodium chloride solution generate solution aerosol. Both released fission products and solution aerosol particles were aspirated by a suction pomp to be transported and mixed in a cylindrical chamber. The volume of chamber is changeable to interact fission products and aerosol particles for different durations. Radioactive aerosol particles were produced by attaching fission products to aerosol particles in the chamber, and the difference of interaction time causes the difference of effective surface area of aerosol particles to attach fission products. The produced radioactive aerosol particles were collected on a polycarbonate filter at downstream of the chamber. The amount of fission products which attaches to aerosol particles were estimated by gamma-ray spectrometry for the filter using a Ge-detector. On the other hand, the amount of fission products released from the irradiated UO_2 powder by heating was estimated by subtraction of gamma-ray spectra measured before and after heating the UO_2 powder.

RESULTS: The attachment ratio of fission products to NaCl solution aerosol particles is shown in Figure 1 as a function of total effective surface area. Squares, triangles and circles show the attachment ratio of ^{95}Zr, ^{103}Ru and ^{131}I, respectively. Diamonds indicate the previous result for ^{104}Tc observed by using ^{252}Cf as a source of fission products. Attachment ratio of ^{104}Tc is larger than those of other isotopes clearly because ^{104}Tc could attach through both processes of electrostatic interaction and collision with recoil velocity. Three kinds of fission product observed in the present work show different attachment ratio each other that indicate the different degree of electrostatic interaction caused by the difference of chemical species.

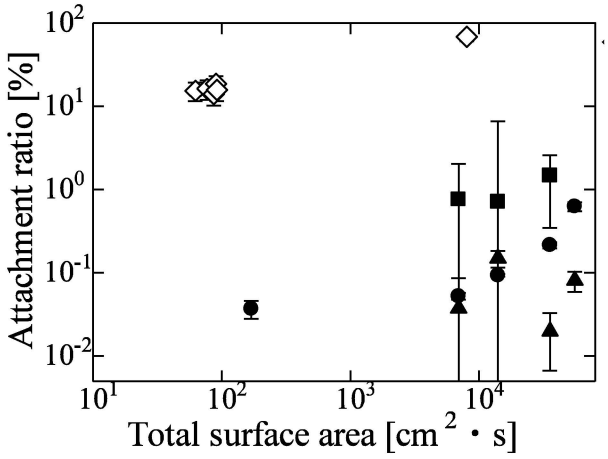

Fig. 1 Attachment ratio of fission products to sodium chloride solution aerosol particles as a function of the total surface area of the aerosol particles.

This work was supported by JSPS KAKENHI Grant Numbers JP24110005 and JP26286076.

REFERENCES:

[1] K. Adachi et al., Scientific Reports, **3** (2013) 2554.
[2] K. Takamiya *et al.,* J. Radioanal. Nucl. Chem. **307** (2016) 2227-2230.
[3] K. Takamiya *et al.,* J Radiat. Prot. Res. **41** (2016) 350–353.
[4] K. Takamiya *et al.,* KURRI Progress Report 2016 (2017) 45-45.
[5] K. Takamiya *et al.,* KURRI Progress Report 2017 (2018) 13-13.
[6] K. Takamiya *et al.,* KURNS Progress Report 2018 (2019) 95-95.

CO9-9 Precipitation of alkaline earth elements toward the chemical study of Nobelium

S. Hayami, Y. Kasamatsu, K. Tonai, E. Watanabe, K. Takamiya[1] and A. Shinohara

Graduate School of Science, Osaka University
[1]Institute for Integrated Radiation and Nuclear Science, Kyoto University

INTRODUCTION: Nobelium (No) with atomic number 102 is one of actinide elements. It is reported that stable oxidation state of No is +2 although those of the other heavy actinide elements are all +3. The chemical behavior of No is reported to be similar to that of group 2 elements in HCl [1]. However, it is difficult to investigate the chemical properties of No because of low production rates and short half-lives of the No nuclides. Therefore, it is important to conduct fundamental experiments of Group 2 elements for chemistry of No.

Previously we reported new experimental method in which the hydroxide complexation of the target elements can be studied from the coprecipitation behavior with samarium hydroxide [2]. So far, we have qualitatively investigated the coprecipitation behaviors of various elements, and we successfully applied the method to element 104, rutherfordium (Rf). Recently, coprecipitation experiments with group 2 elements that are comparative elements for No have been in progress. In this study, both coprecipitation and precipitation experiments were performed for Group 2 elements Ca, Sr, and Ba. In addition, in order to elucidate the new chemical properties of No, we focused on the reaction with sulfate ions, and conducted experiments on coprecipitation behavior of these elements with $BaSO_4$ using ammonium sulfate in addition to sulfate precipitation experiments.

EXPERIMENTS: ^{85}Sr and ^{133}Ba samples were prepared by irradiating protons on pellet samples of RbCl for 1 h and of CsCl for 10 h using the AVF cyclotron at RCNP. ^{47}Ca sample was prepared by irradiating thermal neutrons (3×10^{13} cm^{-2} s^{-1}) on a powder sample of CaO for 1 h using the reactor at KUR. They were separated from other majority of radioisotopes by cation-exchange and anion-exchange methods.

In the hydroxide coprecipitation experiment, 20 μL (20 μg) of Sm standard solution (1 M HNO_3) was added into the ^{85}Sr or ^{133}Ba solution. In case of the precipitation experiment, 20-1000 μg of Sr or Ba chloride or 10 mg of ^{47}CaO in aqueous solution was added. After mixing it, 2 mL of basic solution was added to generate hydroxide precipitate. In the present experiment, we used dilute or concentrated NH_3 solution, or 0.1, 1, or 6 M NaOH solution as the basic solution to observe the dependence of the precipitation yield on the concentration of the basic solution.

In the sulfate coprecipitation experiment, 20 μL (20 μg) of $BaCl_2$ solution was added to the ^{85}Sr or ^{133}Ba solution. In case of precipitation experiment, 20-1000 μg of Sr or Ba chloride solution was added. After mixing it, 2 mL of 0.01, 0.1, or 1.0 M $(NH_4)_2SO_4$ solution was added to generate sulfate precipitate. These solutions were stirred for 5 min at room temperature. The precipitates were collected with membrane filter by suction filtration. The precipitate and filtrate samples were then dried on heater at 100 degree C and were assayed bu γ-ray measurements. The coprecipitation yields were determined from radioactivity of the γ-ray measurements.

RESULTS: The precipitation (ppt) and coprecipitation (co-ppt) yields were determined from the equation: A_{ppt} / ($A_{ppt}+A_{fil}$), where A represents the radioactivity, and ppt and fil indicate the precipitate and filtrate, respectively.

In the hydroxide precipitation and coprecipitation experiment, the yields of precipitation of Ca, Sr, and Ba were very low at low [OH^-] and increased in high [OH^-]. However, the yields of coprecipitation of Sr, and Ba were high at low [OH^-] and almost zero at high [OH^-]. These results might be due to the facts that for alkaline earth metal elements, formation of polynuclear precipitates and species were reported in macro scale. Coprecipitation behavior is considered to relate to the behavior in a mononuclear precipitate. Since the No can be dealt as single atoms, the data on coprecipitation behavior would be able to be used as comparative data to discuss the complex formation of No.

In the sulfate precipitation and coprecipitation experiments (Fig.1), it was found that the coprecipitation behavior of Sr and Ba was basically consistent with that in precipitation. Differences were also found in the coprecipitation yields among group 2 elements which are qualitatively consistent with their solubility products.

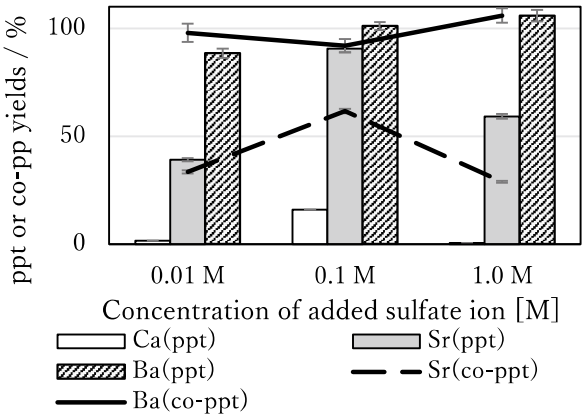

Fig. 1. The yields in sulfate precipitation and coprecipitation experiments.

REFERENCES:

[1] R. J. Silva *et al.*, J. Inorg. Chem., **13**, 9, 2233-2237 (1974).
[2] Y. Kasamatsu, *et al.*, Appl. Radiat. Isot. **118**, 105-116 (2016).